Marchenko Without Up/Down Decomposition on the Marmousi Model and Retrieval of the Refracted Waves: Are They Caused by the Marchenko Algorithm?

Mert S. R. Kiraz & Roel Snieder, Center for Wave Phenomena, Colorado School of Mines
Kees Wapenaar, Delft University of Technology

SUMMARY

Marchenko algorithms retrieve the Green's function for arbitrary subsurface locations, and the retrieved Green's function includes the primary and multiple reflected waves. The Marchenko algorithms require the estimate of the direct arrivals and the reflected waves; however, most previous Marchenko algorithms also require the up/down components of the Marchenko equation for the Green's function retrieval. We use the Marmousi model to retrieve the Green's function without using the up/-down components of the Marchenko equation and show that the retrieved Green's function matches with the numerically modeled Green's function. We also show that the refracted waves can be successfully produced independently from the acquisition geometry, i.e., single-sided or two-sided; however, the retrieval of refracted waves that arrive before the first primary waves is inconsistent with the requirement that the Green's function vanishes before the direct wave. Even though we retrieve such refracted waves, they are caused by the injection of the direct wave into sufficiently detailed background velocity and density models instead of operations of the Marchenko algorithm on the recorded wavefields.

INTRODUCTION

The Marchenko equation was first introduced by the inverse scattering community to make the connection between the scattered data and the scattering potential, as well as medium reconstruction (Newton, 1980; Burridge, 1980; Chadan and Sabatier, 1989; Gladwell, 1993; Colton and Kress, 1998). Rose (2001, 2002) utilizes the Marchenko equation for focusing and shows that the solution of the Marchenko equation creates an incident wavefield which at $t = 0$ becomes a delta function at a prescribed focusing location. Broggini and Snieder (2012) make the single-sided autofocusing concept applicable to the seismic exploration studies, and show that we can focus the wavefield inside the unknown medium using the surface-recorded waves. They also make the connection between the Marchenko equation and seismic interferometry (Weaver and Lobkis, 2001; Wapenaar et al., 2005) and show that the Green's function can be retrieved without illumination from both sides and without a physical receiver at the virtual source location. Following this, Wapenaar et al. (2013) retrieve the three dimensional Green's function and provide a two dimensional example of the Green's function retrieval. Wapenaar et al. (2013) introduce up/down decomposition of the Marchenko equation which constraints the

limitations of the Marchenko equation. The up/down decomposition assumes that the wavefield at the focal point propagates only in the up-down direction; therefore, the algorithm does not work well at large offsets in layered media where refracted waves and near-surface inhomogeneity zones exist.
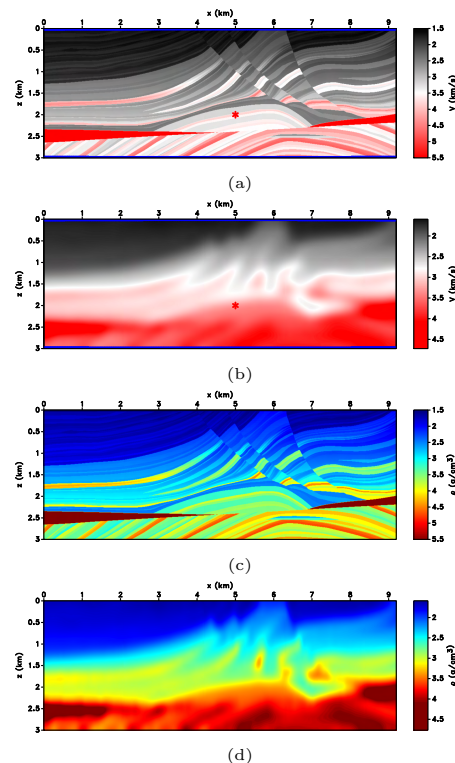

Figure 1: (a) Source and receiver configuration in the Marmousi velocity model. The red asterisk shows the virtual source location and the blue lines show the receiver locations in the subsurface. (b) Smooth version of the Marmousi velocity model. (c) Density model. (d) Smooth version of the density model.

Recently, there have been several studies to address the limitation of the Marchenko method due to the up-/down separation of the Marchenko equation. Kiraz et al. (2020) show wavefield focusing for an arbitrary point inside an unknown highly scattering inhomogeneous medium where we have access to the data acquired on a closed boundary. They show that the Green's function for an arbitrary location in the medium can be retrieved and the retrieved Green's function contains all the scattering effects of the medium, including primary and multiple events. They also show that

the Marchenko focusing without up/down decomposition provides better focusing than the direct wave injection focusing. Diekmann and Vasconcelos (2021) and Wapenaar et al. (2021) present alternative approaches to Green's function retrieval without up/down decomposition for single-sided acquisition, each with their own pros and cons.
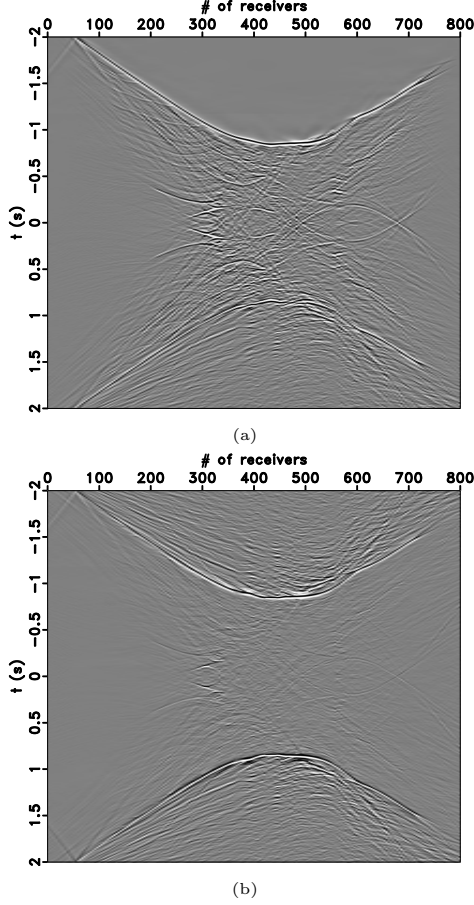

(a)

(b)

Figure 2: (a) $U_{total}(\mathbf{x}, t)$ for the fourth iteration. (b) $U_{total}(\mathbf{x}, t) - U_{total}(\mathbf{x}, -t)$ for the fourth iteration.

We present and discuss a new approach to retrieve the full Green's function at an arbitrary depth location in a complicated medium with a series of normal faults, tilted blocks, horizontally layered horizons, variable velocity, and variable density profiles. We extend the algorithm of Rose (2001, 2002) to two dimensions where we have access to the two-sided illumination and we show that we can circumvent the up/down component separation of the Marchenko equation to retrieve the full Green's function. We present our numerical examples using the Marmousi model for the two-sided illumination where velocity and density are varying for the Green's function retrieval. We compare the numerically modeled Green's function to those obtained from the proposed iterative algorithm and present 2D numerical examples. We also show that we can produce the

refracted waves caused by the complexity of the Marmousi velocity model but their existence only depends on the correctness of the initial estimates of the velocity and density models. By presenting 2D numerical experiments, we show that the retrieved refracted waves have nothing to do with the iterative Marchenko algorithm both in one-sided and two-sided illumination cases; they only depend on the background velocity and density models.
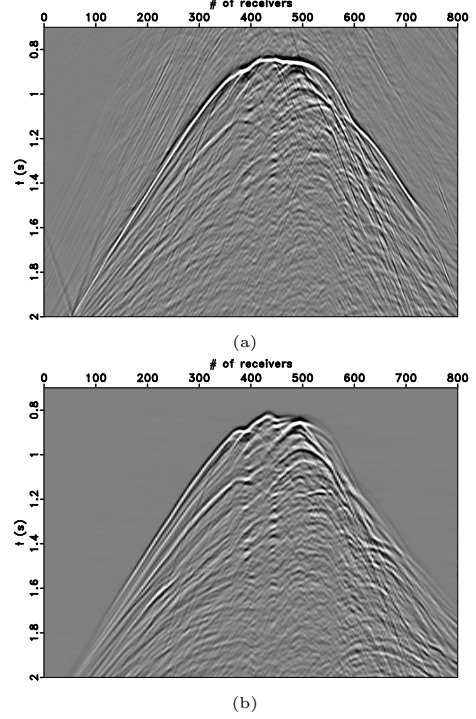

(a)

(b)

Figure 3: (a) The retrieved Green's function using the iterative algorithm. (b) The numerically modeled Green's function.

NUMERICAL EXAMPLE AND GREEN'S FUNCTION RETRIEVAL

Kiraz et al. (2020) give the details of the Marchenko algorithm without up/down decomposition. While the examples they use assume a recording array on a closed surface, and constant velocity and variable density, we show that the same iterative algorithm can, in practice, be applied to the two-sided illumination with variable velocity, and density models. Figure 1a shows the Marmousi velocity model and the source and receiver geometry of our numerical experiment. The red asterisk in Figure 1a denotes the virtual source location and blue lines located at the upper and lower boundaries of the model represent the receiver locations. The virtual source location is given by $x_s = 5$ km and $z_s = 2$ km in depth. Figure 1c shows the variable density model used for the numerical example and Figure 1d shows

the smooth version of the density model. We use finite-difference modeling with absorbing boundaries where surface-related multiples are excluded in the modeling. The source wavelet is a Ricker with a central frequency of 30 Hz.
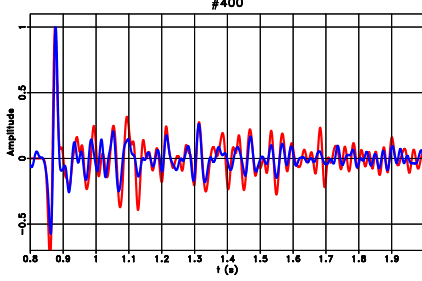

Figure 4: Comparison of the 400th normalized trace of the retrieved Green's function (blue line) and the numerically modeled Green's function (red line).

For this numerical simulation, we use the two-sided data and only show the wavefield recorded at the upper receiver array in Figure 1, and we start the iterative scheme by modeling the direct wave using the smooth version of the velocity and the density models given in Figures 1b and 1d, respectively, for the virtual source location denoted with the red asterisk. We use the modeled direct wave which is ingoing when injected into the medium from the receiver arrays, and use the iterative algorithm to define the outgoing wavefield. Figure 2a shows the superposition of the ingoing wavefield and the outgoing wavefield as $U^{total}(\mathbf{x}, t) = U^{in}(\mathbf{x}, t) + U^{out}(\mathbf{x}, t)$ for the fourth iteration. The wavefield in Figure 2a is symmetric in time, defined using the arrival time of the direct arrival, for $-t_d < t < t_d$ (approximately between the tips of the direct arrivals at -1s and 1s). If we take the difference between the total wavefield in Figure 2a and its time-reversed version, i.e., $U_{dif} = U_{total}(\mathbf{x}, t) - U_{total}(\mathbf{x}, -t)$, all events in the interval $-t_d < t < t_d$ vanish as shown in Figure 2b. Figure 2a shows that the wavefield is symmetric in time for $-t_d < t < t_d$, hence in Figure 2b they vanish in this interval. Although some energy remains in Figure 2b for $-t_d < t < t_d$, this is due to numerical inaccuracies in our solution of the Marchenko equation.

The difference wavefield U_{dif} enables us to create the response to a virtual source located in the subsurface at the focal point without using the up/down decomposition of the Marchenko equation. Figure 3a shows U_{dif} for the fourth iteration for positive times only and Figure 3b shows the numerically modeled Green's function for the virtual source location. The retrieved Green's function in Figure 3a matches with the numerically modeled Green's function in Figure 3b for $t > t_d$; however, the retrieved direct waves do not include the refracted waves shown between the receiver numbers 500 and 700. This is due to the smooth version of the velocity and density models used for the iterative scheme that is too

smooth to produce refracted waves. Figure 4 shows the normalized trace comparison of the estimated and true Green's functions for the receiver number 400 for positive times only to emphasize the similarities between the retrieved and modeled Green's function. As a result of our iterative solution, we retrieve the direct wave and multiply-scattered wave information, and directly modeled and retrieved Green's functions match both in time and amplitude.

DISCUSSION

Figure 2b shows that for positive times, the wavefield $U_{total}(\mathbf{x}, t) - U_{total}(\mathbf{x}, -t)$ vanishes at the receivers for $-t_d < t < t_d$. If we consider this wavefield at $t = 0$, the direct waves radiated at $t = 0$ from $\mathbf{x}_s$ arrive at a receiver location $\mathbf{x}_R$ at t_d. If we suppose that waves would radiate at $t = 0$ from a point $\mathbf{x} \neq \mathbf{x}_s$, for some receivers, those waves would arrive at a time $t < t_d$; however, as shown in Figure 2b, no waves arrive at time $t < t_d$. This means that waves do not radiate from any point $\mathbf{x} \neq \mathbf{x}_s$ at $t = 0$, and the retrieved Green's function therefore is, up to a multiplicative constant, the Green's function.

The retrieved Green's function shown for positive times only in Figure 3a matches with the numerically modeled Green's function in Figure 3b except for the refracted waves, and Figure 4 shows that the Marchenko algorithm without up/down decomposition retrieves the primary and multiple events for the variable velocity and density Marmousi model. However, because we inject the wavefield from a limited aperture (blue lines in Figure 1) back into the medium in the iterative process, we use a cosine taper on both right and left edges of the wavefield to suppress truncation artefacts. Therefore, the right and left sides of the retrieved Green's function are reduced by the taper, leading to a poor match of the retrieved and the modeled Green's function around the edges of the receiver aperture.

The major difference between the retrieved and the modeled Green's function can be seen around the direct arrivals. The modeled Green's function in Figure 3b shows that due to the virtual source location and complexity of the medium, refracted waves are present in the recorded Green's function; however, the retrieved Green's function in Figure 3a does not include the refracted waves around the direct arrivals. The lack of the refracted waves in the retrieved Green's function is due to the smoothness of the velocity and density models used to model the direct arrivals. For comparison, Figures 5a and 5b show less smooth version of the velocity and density models, respectively, than the one we use in the iterative process for the same source and receiver locations. Using these velocity and density models, Figure 5c shows the retrieved Green's function without up/-down decomposition and the labels R1, R2, and R3 in Figure 5c show the observed refracted waves which are

not present in Figure 3a. We see that both retrieved Green's functions in Figures 3a and 5c, are similar to each other for times when $t > t_d$. This indicates that the proposed Marchenko algorithm without up/down decomposition retrieves the primaries and multiples; however, the retrieved refracted waves do not come from the Marchenko iterations but depend on the spatial variations of the velocity and density models used to model the direct arrivals.
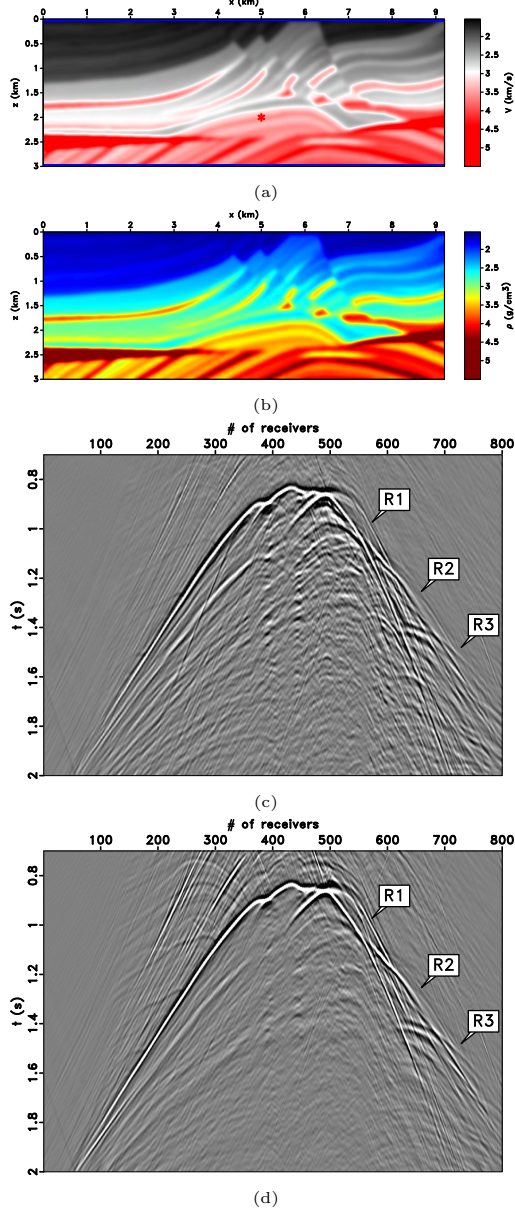

(a)

(b)

(c)

(d)

Figure 5: (a) Smooth version of the velocity model. (b) Smooth version of the density model. (c) The retrieved Green's function. (d) The retrieved Green's function using only the upper acquisition boundary.

The one-sided illumination does suffice to include the refracted waves using a less smooth version of the ve-

locity and density models. Figure 5d shows an estimate of the Green's function from the direct wave injection only from the upper acquisition boundary (upper blue line) in Figure 5a and the labels R1, R2, and R3 denote the recorded refracted waves. The refracted waves are present despite the single-sided acquisition and despite the fact that the direct wave injection does not include any iterations of the Marchenko algorithm. Figure 5d shows that the refracted waves depend only on the initial estimates of the velocity and density models and on the injection of the direct wave. The acquisition boundary, either one-sided or two-sided, and the iterations of the Marchenko algorithm do not affect the observed refracted waves. Figure 5d also shows that the refracted waves even with the direct wave injection match well with the numerically modeled refracted waves (see Figure 3b). The direct wave injection produces the refracted waves and this shows that the retrieval of these refracted waves is not the result of the Marchenko algorithm. While these observations still require further investigation, we claim that the accurateness of the refracted waves in this experiment depends only on the initial estimate of the velocity and density models, rather than on the iterative processing of recorded waves in the Marchenko algorithm.

CONCLUSIONS

We present the Green's function retrieval without up-/down decomposition using the Marmousi model. We show that we can retrieve the Green's function for an arbitrary depth location independent of the medium complexity. Our retrieved Green's function retrieves both the primary and multiple events of the heterogeneous subsurface model. We also successfully produce the refracted waves in the retrieved Green's function when detailed velocity and density information are available for the initial estimate of the direct waves. We compare the effects of the background velocity and density models for one-sided and two-sided illumination on producing the refracted waves. Our results show that the observed refracted waves only depend on the initial estimates of the velocity and density models, and are not a result of the Marchenko algorithm. The refracted waves can be produced even at the first iteration when the velocity and density models have detailed information about the subsurface, these refracted waves do not arise because of the iterative Marchenko algorithm.

ACKNOWLEDGMENTS

REFERENCES

Broggini, F., and R. Snieder, 2012, Connection of scattering principles: A visual and mathematical tour: European Journal of Physics, **33**, no. 3, 593–613.

Burridge, R., 1980, The gelfand-levitan, the marchenko, and the gopinath-sondhi integral equations of inverse scattering theory, regarded in the context of inverse impulse-response problems: Wave Motion, **2**, 305–323.

Chadan, K., and P. C. Sabatier, 1989, Inverse problems in quantum scattering theory: Springer.

Colton, D., and R. Kress, 1998, Inverse acoustic and electromagnetic scattering theory: Springer.

Diekmann, L., and I. Vasconcelos, 2021, Focusing and green's function retrieval in three-dimensional inverse scattering revisited: A single-sided marchenko integral for the full wave field: Phys. Rev. Research, **3**, no. 1, 013206.

Gladwell, G. M. L., 1993, Inverse problems in scattering: Kluwer Academic Publishing.

Kiraz, M. S. R., R. Snieder, and K. Wapenaar, 2020, Marchenko focusing without up/down decomposition: SEG Technical Program Expanded Abstracts 2020, 3593–3597.

Newton, R. G., 1980, Inverse scattering. I. one dimension: Journal of Mathematical Physics, **21**, 493–505.

Rose, J. H., 2001, "Single-sided" focusing of the time-dependent Schrödinger equation: Physical Review A, **65**, no. 1, 012707.

———, 2002, Time reversal, focusing and exact inverse scattering. in: Fink m., kuperman w.a., montagner jp., tourin a. (eds) imaging of complex media with acoustic and seismic waves. topics in applied physics, vol 84: Springer, Berlin, Heidelberg.

Wapenaar, K., F. Broggini, E. Slob, and R. Snieder, 2013, Three-dimensional single-sided marchenko inverse scattering, data-driven focusing, green's function retrieval, and their mutual relations: Phys. Rev. Lett., **110**, no. 8, 084301.

Wapenaar, K., J. Fokkema, and R. Snieder, 2005, Retrieving the Green's function in an open system by cross correlation: A comparison of approaches (L): The Journal of the Acoustical Society of America, **118**, no. 5, 2783–2786.

Wapenaar, K., R. Snieder, S. de Ridder, and E. Slob, 2021, Green's function representations for marchenko imaging without up/down decomposition: arXiv:2103.07734.

Weaver, R., and O. Lobkis, 2001, Ultrasonics without a source: Thermal fluctuation correlations at MHz frequencies: Physical Review Letters, **87**, no. 13, 134301.